# Variable gearing in pennate muscles

**Emanuel Azizi*, Elizabeth L. Brainerd, and Thomas J. Roberts**

Department of Ecology and Evolutionary Biology, Brown University, Providence, RI 02912

Edited by Ewald R. Weibel, University of Bern, Bern, Switzerland, and approved December 3, 2007 (received for review September 27, 2007)

**Muscle fiber architecture, i.e., the physical arrangement of fibers within a muscle, is an important determinant of a muscle's mechanical function. In pennate muscles, fibers are oriented at an angle to the muscle's line of action and rotate as they shorten, becoming more oblique such that the fraction of force directed along the muscle's line of action decreases throughout a contraction. Fiber rotation decreases a muscle's output force but increases output velocity by allowing the muscle to function at a higher gear ratio (muscle velocity/fiber velocity). The magnitude of fiber rotation, and therefore gear ratio, depends on how the muscle changes shape in the dimensions orthogonal to the muscle's line of action. Here, we show that gear ratio is not fixed for a given muscle but decreases significantly with the force of contraction ($P < 0.0001$). We find that dynamic muscle-shape changes promote fiber rotation at low forces and resist fiber rotation at high forces. As a result, gearing varies automatically with the load, to favor velocity output during low-load contractions and force output for contractions against high loads. Therefore, muscle-shape changes act as an automatic transmission system allowing a pennate muscle to shift from a high gear during rapid contractions to low gear during forceful contractions. These results suggest that variable gearing in pennate muscles provides a mechanism to modulate muscle performance during mechanically diverse functions.**

biomechanics | force–velocity tradeoff | gear ratio | muscle architecture

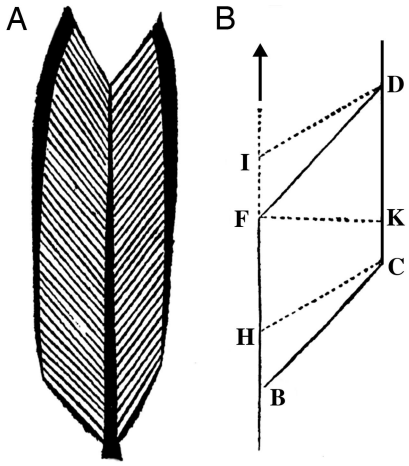


**Fig. 1.** A 17th century geometric examination of muscle architecture (5). (*A*) The adductor muscle in the claw of a lobster exemplifies bipennate architecture. (*B*) A geometric model of a unipennate muscle highlighting the orientation of fibers at rest (BC and DF) and contracted (HC and ID). This classic model predicts a change in pennation angle (i.e., fiber rotation) during contraction and assumes that muscle thickness (FK) remains constant. Arrow indicates the direction of the muscles' lines of action. Modified from reference 5.

The force, speed, and power that can be harnessed from skeletal muscles to power movement are ultimately limited by the mechanical behavior of myofibers, the muscles' contractile cells. Two features of the contractile behavior of myofibers that likely constrain locomotor performance are the well defined limits to contraction velocity and contractile force. The maximum shortening velocity of a myofiber can be characterized by allowing the muscle to contract against near-zero loads, and a maximum isometric force can be defined when a muscle contracts at a fixed length. To understand how these limits to speed and force at the level of skeletal muscle cells translate to limits to speed or force of movement requires a consideration of musculoskeletal components that modulate force and velocity "downstream" of the force-producing cells. The most familiar of these are the skeletal lever systems, which define the mechanical advantage (gearing) through which muscle force is transmitted (1, 2). Like any lever or gear, skeletal gearing influences the ratio of muscle force or velocity to output force or velocity.

A less obvious potential gearing mechanism resides within the architecture of the muscles themselves (3). It is generally recognized that skeletal muscle architecture influences the force and velocity of a muscle, but in most cases, the analysis of the effects of muscle architecture on force or velocity output has been limited to predictions based on static anatomy. Dynamic changes in muscle architecture during a contraction have the potential to alter the gearing through which muscle fibers operate and, therefore, maximum muscle force and velocity output; but this feature of muscle architecture is largely unexplored.

In many skeletal muscles, the force-generating fibers are oriented at an angle relative to the muscle's line of action (4). The arrangement of fibers and tendons in these muscles resembles the veins and rachis of a bird feather, leading to the designation of such muscles as pennate (from Latin "penna" or feather; Fig. 1*A*). The advantage of this arrangement, first appreciated by anatomists >300 years ago (5), is that more fibers can be packed into a given volume of muscle, and thus the force of a pennate muscle is greater than a parallel-fibered muscle of equal volume (6). It has long been recognized that there are two tradeoffs associated with pennate muscle architecture. First, the oblique orientation of pennate muscle fibers means that only the component of fiber force oriented along the muscle's line of action can contribute to whole-muscle force (4). Second, pennate muscles have shorter muscle fibers, and with fewer sarcomeres in series, their displacements and velocities are low compared with longer-fibered parallel muscles (7).

The reduction in total shortening velocity associated with shorter muscle fibers is offset in part by the dynamic effects of fiber shortening in a pennate muscle. When fibers in a pennate muscle shorten, they rotate to greater angles of pennation (Fig. 1*B*) (5, 8–10). As a result, the muscle's velocity along its line of action can exceed the velocity of the contracting fibers (3, 8, 10). This velocity amplification can be measured as the ratio of muscle fiber velocity to whole-muscle velocity, a relationship that describes a muscle's architectural gear ratio (AGR). The ampli-

Author contributions: E.A., E.L.B., and T.J.R. designed research; E.A. and T.J.R. performed research; E.A. analyzed data; and E.A., E.L.B., and T.J.R. wrote the paper.

The authors declare no conflict of interest.

This article is a PNAS Direct Submission.

*To whom correspondence should be addressed at: Department of Ecology and Evolutionary Biology, Box G B-204, Brown University. E-mail: manny_azizi@brown.edu.

This article contains supporting information online at www.pnas.org/cgi/content/full/0709212105/DC1.

fying effects of changes in fiber pennation angle (i.e., fiber rotation) with shortening generally result in AGRs >1 (3).

A recent analysis of muscle architecture predicts that AGR can vary depending on the relative magnitude of muscle-shape changes in the directions orthogonal to the muscle's line of action (3). Some degree of orthogonal shape change is necessary in any contracting muscle because total muscle volume must remain constant (11) while fibers decrease in length and increase in diameter. The shortening of muscle fibers must therefore be accommodated by bulging of the muscle in one or more orthogonal directions. The significance of dynamic changes in muscle shape has been overlooked in most classic models of pennate muscle (12). Most commonly it is assumed that the distance between two aponeurotic sheets (muscle thickness; FK in Fig. 1) remains constant during a contraction (4, 13). This assumption has obscured the potential effect of muscle shape changes and has been challenged by recent empirical studies that demonstrate changes in muscle thickness in some muscles during contraction (9, 14–17).

A three-dimensional pennate muscle simulation illustrates how the direction of bulging in a muscle can influence gearing (Fig. 2). If fiber shortening is largely accommodated by an increase in muscle thickness (i.e., the distance between aponeuroses increases; Fig. 2*B*), then the pennation angle increases substantially as fibers shorten, resulting in more shortening of the muscle tendon unit and a high AGR. In contrast, fibers could shorten without rotating if there were sufficient decrease in muscle thickness during a contraction (Fig. 2*C*). This could occur if the muscle bulged in width rather than thickness. This condition is less favorable for velocity because it lacks the velocity-amplifying effects of fiber rotation, but it is favorable for force production because the pennation angle does not increase with fiber shortening. Any increase in pennation angle decreases muscle force output because it reduces the component of fiber force oriented along the muscle's line of action. The two extremes of muscle-shape change represented in Fig. 2 illustrate that shape changes could favor either force or velocity during contraction in a pennate muscle.

In this study, we measure the effect of muscle-shape changes on architectural gear ratio in a contracting pennate muscle. Our model system is an *in situ* preparation of the lateral gastrocnemius (LG) of the wild turkey (*Meleagris gallopavo*), a unipennate muscle with an average pennation angle of 25°. If this muscle maintains a constant thickness during contraction, as assumed by most models of muscle architecture (4, 13), it should operate with a gear ratio of ≈1.2. Alternatively, higher (favoring velocity) or lower (favoring force) gear ratios would be expected if muscle thickness increases or decreases (Fig. 2). To isolate the effects of muscle-shape changes on gearing, we performed a series of isotonic contractions at varying levels of force while keeping the initial fiber length, initial pennation angle, and total fiber strain constant. During each contraction, measurements were taken when force was constant to control for the potential confounding effects of stretching series elastic elements (see *Materials and Methods* for detail). We determined the AGR by independently measuring muscle fiber velocity using sonomicrometry and whole-muscle velocity using a servomotor during a series of isotonic contractions (Fig. 3). We also used sonomicrometry to quantify instantaneous muscle thickness and pennation angle during each contraction (Fig. 3).

## Results

During nearly all contractions, the shortening velocity of the muscle–tendon unit exceeded the shortening velocity of the fiber during isotonic force production, as illustrated in representative contractions (Fig. 3 *B* and *F*). Instantaneous pennation angle consistently increased throughout the period of contraction (Fig. 3 *C* and *G*). Muscle thickness (the distance between deep and superficial surfaces of the muscle) also changed over the course of a contraction. However, the magnitude and direction of change in muscle thickness varied between contractions depending on the magnitude of force production. In low-force contractions, thickness increased as fibers shortened, whereas during high-force contractions, muscle thickness decreased (Fig. 3 *D* and *H*).

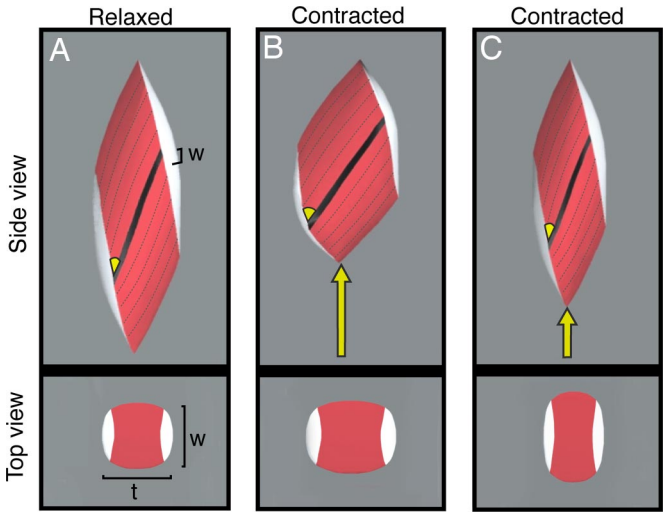


**Fig. 2.** Simulations of an isovolumetric, three-dimensional unipennate muscle. (*A*) Virtual pennate muscle shown at rest in side and top view. The muscle belly is shown in red, and the aponeuroses are shown in white. Muscle thickness (t) and muscle width (w) define the two directions orthogonal to the line of action. (*B*) A simulation in which muscle thickness increases as fibers shorten by 13% of resting length. An increase in muscle thickness results in substantial fiber rotation and a large amount of muscle shortening (yellow arrow). This simulated shape change results in a relatively high gear ratio that would favor the velocity output of a muscle. (*C*) A simulation in which muscle thickness decreases as the fibers shorten by 13% of resting length. A decrease in muscle thickness counteracts fiber rotation and results in relatively little muscle shortening (compare yellow arrows in *B* and *C*). This simulated shape change results in a relatively low gear ratio and less fiber rotation that would favor muscle force production. These simulations represent extremes along a continuum of potential shape changes and highlight how dynamic shape changes during a contraction can significantly alter the force and velocity output of a pennate muscle.

The trends apparent in the representative contractions in Fig. 3 are confirmed by data pooled for all individuals over a range of contractile force levels. There was a systematic negative relationship between the change in muscle thickness and muscle force ($P < 0.0001$; Fig. 4*A*). Muscle thickness increased during low-force contractions and decreased during high-force contractions. Measurements of fiber rotation were consistent with the prediction from simulations that the magnitude of thickness increase and the magnitude of fiber rotation should be correlated. Fibers rotated (i.e., increased their angle of pennation) the most in low-force contractions, and the degree of fiber rotation declined systematically with increasing levels of force ($P < 0.0001$; Fig. 4*B*). As a result of variable shape changes across force levels, the muscle could not be characterized by a single AGR but rather showed a significant decrease in AGR across contractions at different levels of force ($P < 0.0001$; Fig. 4*C*). The value of gear ratio had a substantial effect on the relative shortening velocity of the muscle relative to that of the fiber. Architectural gear ratios for low-force contractions indicate that muscle velocity is amplified by nearly 40% (AGR = 1.4) for low-force contractions, whereas at high-force levels, muscle fascicle velocity and muscle velocity are approximately equal (AGR ≈ 1).

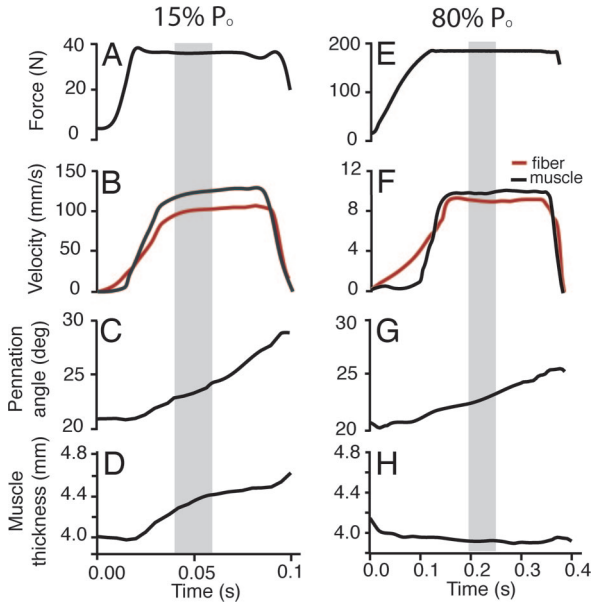


**Fig. 3.** Representative isotonic contractions in the lateral gastrocnemius of the wild turkey. The muscle was maximally stimulated in a branch of the sciatic nerve. Time-series plots from two sample contractions are shown. Muscle force was allowed to increase to a preset level (15% of maximum isometric force ($P_o$) in *A–D* and 80% $P_o$ in *E–H*) and was kept constant as the muscle fiber (red) and the muscle–tendon unit (black) shortened at a constant velocity. All measurements were taken during a period of constant force (gray bars) and at a similar initial pennation angle. Similar contractions were performed at varying levels of force for each muscle.

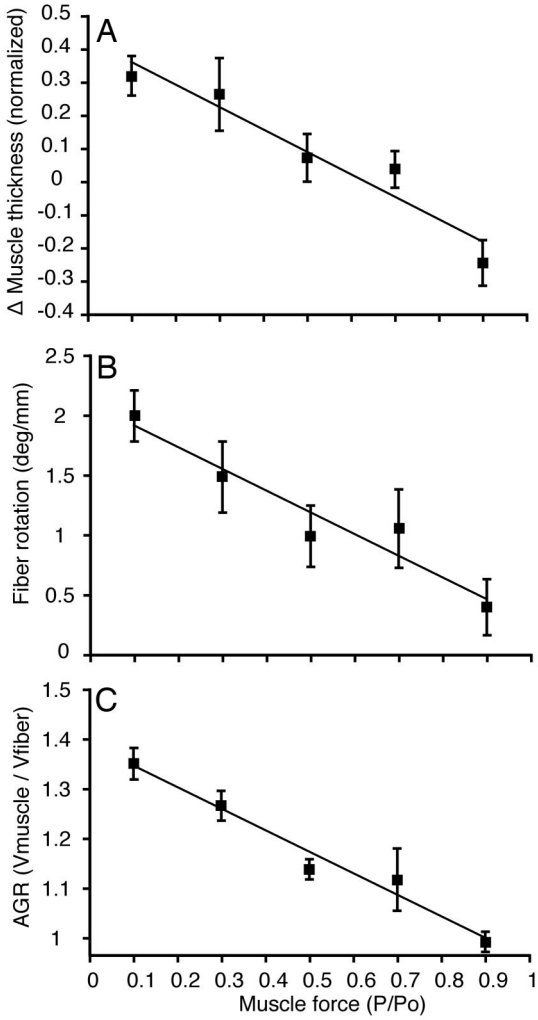


**Fig. 4.** Change in muscle thickness, fiber rotation, and architectural gear ratio (AGR) during a series of isotonic contractions at different force levels (*P*, expressed as a fraction of maximum isometric force, $P_o$). (*A*) The change in muscle thickness per millimeter of fiber shortening decreased as we increased the force level of the isotonic contractions (least-squares regression; $P < 0.0001$). During low-force, high-velocity contractions, muscle thickness increases (positive values), whereas at high forces, muscle thickness decreases (negative values). (*B*) The magnitude of fiber rotation per millimeter of fiber shortening decreases as contractions become more forceful (least-squares regression; $P < 0.0001$). (*C*) Architectural gear ratio (muscle velocity/fiber velocity) is lower for contractions at higher force levels (least-squares regression; $P < 0.0001$). The muscle operates with a gear ratio that favors velocity during low-force, high-velocity contractions and shifts to a gear ratio that favors force during slow, forceful contractions. Values are mean ± SE; $n = 4$ individuals.

In this study, we controlled muscle force and allowed fiber-shortening velocity to vary according to the intrinsic force–velocity relationship. Therefore, in our experimental design, force and velocity covary between contractions such that high-force contractions correspond to lower shortening velocities and low-force contractions correspond to high shortening velocities. This experimental design leaves open the possibility that our measured decrease in AGR resulted from lower contraction velocities rather than higher muscle forces. To test this alternate interpretation, we used a contraction protocol in which muscle fatigue resulted in variable force at the same shortening velocity (Fig. 5). We find that, even at a constant shortening velocity, AGR decreases significantly with increasing force ($P < 0.0001$). These measurements decoupled the effects of force and velocity and confirm our conclusion that variation in muscle force alters the muscle's gear ratio.

## Discussion

In traditional pennate muscle models, the distance between aponeurotic sheets (muscle thickness) is held constant during simulated contraction (4, 13). For our turkey lateral gastrocnemius muscle with an initial pennation angle of 25°, these models predict a fixed gear ratio of 1.2. In our results, a range of gear ratios were observed, so this prediction is not supported. What is surprising in these results is not that gear ratio departs from a value of 1.2 but that it is variable. Architectural gear ratio is high during low-force, high-velocity contractions and low during high-force, low-velocity contractions. This variation in AGR appears to be mediated by muscle-shape changes that are variable, depending on the level of force developed in a contraction.

The variable gearing observed in our measurements may represent a previously unrecognized mechanism for improving muscle performance over a range of mechanical demands. Force and movement are transmitted from muscle fibers to the skeletal system with a high gear during rapid movements and a low gear during forceful movements. Similar to a cyclist shifting gears to better match the steepness of a hill, variable gearing may allow a pennate muscle to match the output of the muscle motor to the demand for speed or force over a broad range of movements.

It is well known that a fiber's intrinsic force–velocity properties can limit a muscle's range of mechanical output (18, 19). At high shortening velocities, the rate of cross-bridge detachment limits a fiber's capacity for force generation, resulting in the familiar hyperbolic relationship between force and velocity (20). The presence of variable gearing in pennate muscle may serve to extend this range by modulating how the forces and displacements generated by a fiber are transmitted through the muscle–

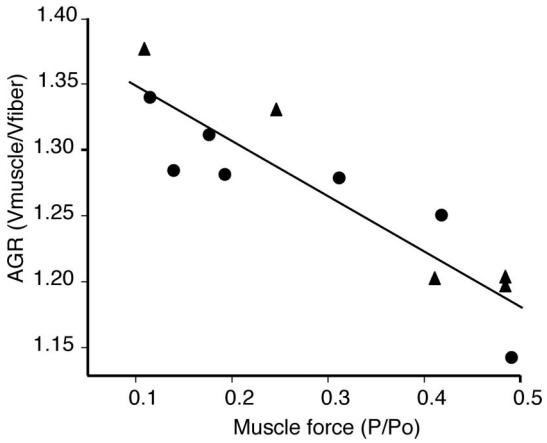


**Fig. 5.** Architectural gear ratio (AGR) plotted against muscle force for a series of isovelocity contractions. Data are shown for contractions performed at the same shortening velocity (23.7 mm/s) but after trains of contractions of different durations. The longer the duration of the preceding train, the more fatigued the muscle and the lower its force output. These results show that, despite a constant shortening velocity, AGR decreased significantly with increasing force (least-squares regression $P < 0.0001$). The pattern observed is similar to that shown for isotonic contractions. Data from two birds are shown as different symbols.

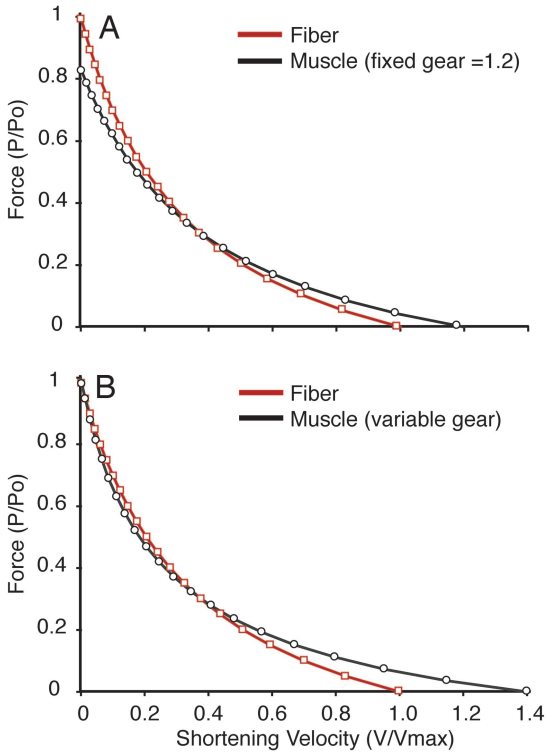


**Fig. 6.** The effect of variable gearing on the functional range of a pennate muscle. The force–velocity properties of a fiber are used to predict the output force and output velocity of a muscle with a fixed gear (*A*) and a variable gear (*B*). The output force and velocity of the whole muscle are expressed in the units of $V/V_{max}$ and $P/P_o$ of the fiber. Muscle power is assumed to be conserved such that the power profiles of all curves are identical. (*A*) In the fixed-gear condition, the muscle is set to operate with a constant gear ratio of 1.2. (*B*) In the variable-gearing condition, the empirical relationship between gear ratio and force (Fig. 4*C*) is used to calculate the whole muscle's force–velocity curve. Variable gearing provides higher whole-muscle force during slow forceful contractions and higher velocity during fast contractions.

tendon system. The effect of variable gearing can be illustrated by comparing the range of outputs expected in the turkey lateral gastrocnemius operating with a constant (Fig. 6*A*) or a variable (Fig. 6*B*) gear ratio. If gear ratio is fixed (1.2 in Fig. 6*A*), there is a consistent offset between force or velocity in the fiber and force or velocity output of the muscle. For a gearing of 1.2, for example, this means that maximal velocities are 20% greater than fiber velocities, but it also means that maximal forces are 20% lower than maximal fiber force (summed across all fibers). If architectural gear ratio is variable, muscle performance can be improved for both fast and forceful contractions. Given the gear ratios observed in the turkey LG, muscle velocity exceeds fiber velocity by nearly 40% for the fastest contractions, whereas the most forceful contractions occur with almost no decrement in summed fiber force (Fig. 6).

To our knowledge, variable gearing in pennate muscles has not been reported previously. Recent advances in musculoskeletal imaging via ultrasound and magnetic resonance have provided detailed images and measurements of both fiber rotation and changes in muscle thickness in human muscles *in vivo* (9, 16, 17). Results from these studies show that muscle thickness can change during pennate muscle contractions. However, it is difficult to determine from currently available data whether these measurements support our finding of a variable gearing. The primary difficulty lies in the covariation of muscle force and fiber strain in the fixed-end contractions that are typically studied. For example, the positive correlation between muscle thickness increase and force that has been reported for fixed-end contractions in triceps surae (9) is seemingly inconsistent with the negative relationship between muscle thickness increase and force reported here (Fig. 4*A*). However, high-force contractions in a fixed-end protocol are also associated with higher total fiber strains (and therefore greater shape changes) as muscle fascicles shorten more against series elastic elements during high-force contractions. Furthermore, force varies over the entire course of these contractions, and therefore net muscle thickness changes may be influenced by shape changes that occur dynamically during the low-force portions of any contraction. In our *in situ* preparations, we isolated the effect of muscle-shape change by making measurements during a period of constant force over approximately the same fiber strains and starting pennation angles.

The effect of variable gearing may be apparent in a previous study of isolated cat muscles, in which muscle fiber velocity and whole-muscle velocity were measured independently in contractions at variable levels of force (21). This study demonstrated a mismatch between fiber velocity and muscle velocity that decreased as the force of contraction increased. The observed mismatch between fiber and muscle velocity was interpreted as a measurement error resulting from an isokinetic experimental protocol (20). Our results suggest an alternative interpretation in which the variable mismatch between fiber velocity and muscle velocity is explained by a force-dependent variable gearing.

Our results suggest that an obliquely oriented muscle fiber can automatically follow different trajectories depending on muscle force. Because this mechanism occurs in an isolated muscle preparation, we can conclude that it is not mediated by nervous control over shape change. We hypothesize that it results from the passive effects of intramuscular forces and pressures on connective tissue elements. For fibers to rotate during shortening, a muscle must resist the component of fiber force perpendicular to the muscle's line of action, which tends to compress the muscle and decrease muscle thickness. Decreases in muscle thickness require increases in muscle width, and we speculate that the resistance of connective tissue elements to increases in muscle width provides this critical control over muscle shape changes (22). At low muscle forces, the resistance to changes in

muscle width may constrain fibers to rotate as they shorten. At high muscle forces, the component of the fiber force perpendicular to the line of action may be sufficient to overcome this resistance to increases in muscle width, and the muscle is compressed as thickness decreases. Previous observations of increases in aponeurosis width during isometric contractions may reflect such shape changes at relatively high forces (23–25). In addition, pennate muscle models have demonstrated that muscles with relatively high pennation angles (as seen in the turkey LG) may generate high intramuscular pressures (26, 27), which may result in substantial shape changes during contraction. We speculate that the variable gearing mechanism observed in this study is ultimately mediated by connective-tissue elements that control the shape changes that alter gearing.

In any motor-driven system, gearing can provide a means of managing the tradeoff between force and velocity inherent in a finite power source. In muscles, the importance of gearing mechanisms has been recognized at multiple levels of organization, from the force–velocity tradeoff defined by lever arms of myosin heads during cross-bridge formation (28) to the action of skeletal lever systems (2). The results presented here highlight a previously unappreciated gearing mechanism that occurs at the level of muscle-fiber architecture. Variable shape changes in pennate muscles during a contraction may effectively provide an automatic transmission system, in which the tradeoff between force and velocity is self-regulated to match the mechanical demands of a contraction.

## Materials and Methods

**Muscle Simulations.** Simulations shown in Fig. 2 represent the first and last frames of animations constructed in the three-dimensional virtual environment Maya (version 7; Autodesk). Muscle shapes are created from basic polygonal objects, and the initial pennation angle of the muscle was set to 25°. The muscle is constrained to shorten along its long axis and allowed to expand in other dimensions to maintain a constant volume. The entire muscle including aponeuroses behaves as a single homogenous object. A range of potential shape changes was explored, but only two extreme conditions are highlighted in Fig. 2. The simulations included only the shortening behavior of the muscle and did not include any kinetic information as model inputs. Any inference regarding the force benefit of different behaviors is based on the changes in the trajectory of the muscle fiber relative to the muscle's line of action. All bulging conditions were compared for the same amount of fiber shortening. See supporting information (SI) Movie 1 to view animation.

***In Situ* Preparation.** The protocols used for this muscle preparation are modified from a previous study (29). We independently measured muscle fiber velocity using sonomicrometry and whole-muscle velocity using a servomotor. In addition, we used sonomicrometry to quantify instantaneous muscle thickness and pennation angle. Muscle force was controlled by a servomotor (Aurora Scientific), such that during each contraction, muscle force was kept constant as the muscle shortened. A series of these isotonic contractions was performed at different levels of force. This experimental protocol allowed us to control for two important factors. First, we controlled for the potentially confounding effects of stretching series elastic elements by measuring the architectural properties of the muscle during a period of constant force. Second, we took measurements at the same initial muscle fiber length and initial pennation angle and total fiber strain for all force conditions to isolate the effects of muscle shape changes on muscle gearing.

Birds were deeply anesthetized with inhaled isoflurane. A branch of the sciatic nerve was isolated and connected to a bipolar stimulating electrode. The lateral gastrocnemius muscle was implanted with three piezoelectric crystals (Sonometrics) to measure fiber length (crystals oriented along the muscle fiber), muscle thickness, and pennation angle during contractions (SI Fig. 7). These transducers were secured in place by using a small drop of Vet-bond skin adhesive. The position of sonomicrometry transducers was confirmed postmortem to ensure that the transducers were aligned along the fascicle axis and to check for potential movement of transducers during the experiment. The leg was fixed to a rigid custom-made aluminum frame by using an aluminum plate that was fastened to the femur by using machine screws. The distal tendon of the muscle was isolated, and the ossified portion of the tendon was clamped to the lever of the servomotor. The ossified tendon provides a secure, rigid and reliable connection with the servomotor.

The muscle was left in its natural position relative the adjacent muscles and the tibiotarsus. Care was taken to limit disruption of the skin and fascial surroundings of the muscle. Muscle temperature was monitored and maintained between 36 and 39°C. All experimental protocols were approved by the Brown University Institutional Animal Care and Use Committee.

Before the tetanic isotonic contractions, the optimum stimulation voltage and fiber length were determined. First, the muscle's twitch force was monitored as the stimulation voltage was increased by 1-V increments. The voltage that resulted in maximum twitch force was increased by 1 V and used to stimulate the muscle maximally. Second, a series of twitches at varying lengths were used to construct a length–tension relationship and determine the optimal operating length of the muscle. All tetanic contractions were started at lengths such that the shortening phase of the contraction encompassed the muscle's optimal length.

Muscles were stimulated supramaximally under isotonic conditions (Grass Instruments). Force was allowed to develop to a preset value and was maintained at a constant level by using a servomotor. During the period of constant force, the muscle shortened at a nearly constant velocity (Fig. 3). The muscle was allowed a minimum of 5 minutes between contractions to prevent fatigue. Each muscle was subjected to approximately 10 contractions ranging in force from 10% to 100% of $P_o$. All measurements were taken over a period of constant force and at approximately the same initial fiber length and pennation angle (Fig. 3).

In a subset of experiments, the muscle was subjected to a series of isovelocity contractions after trains of contraction of varying duration. This protocol allowed us to alter force output by differentially fatiguing the muscle before a contraction. During these isovelocity contractions, the length changes of the muscle were controlled by an external wave inputted to the servomotor. In these contractions, muscle shortening velocity was set to 23.7 mm/s ($\approx$0.15 $V_{max}$). Data from these contractions were used to quantify the muscle's gear ratio at a single shortening velocity but across a range of forces.

Sonomicrometry and servomotor data were acquired as analog signals and recorded at 4,000 Hz by using custom LabView software (version 7.1; National Instruments). In most cases, data did not require significant postprocessing. However, in a few cases, data were smoothed with a quintic spline by using Igor Pro (v.4.0; Wavemetrics).

**Data Analysis and Statistics.** Data from individual contractions were analyzed by using Igor Pro (version 4.0; Wavemetrics). For each individual, the change in muscle thickness, change in pennation angle, and gear ratio were quantified at a range of force levels. Instantaneous muscle-fiber length and muscle thickness were measured directly by pairs of sonomicrometry crystals (SI Fig. 7). Pennation angle was calculated by using the three sides of a triangle formed by the array of sonomicrometry crystals (SI Fig. 7). Changes in muscle thickness and pennation angle were normalized by the amount of muscle-fiber shortening (Fig. 4*A*and *B*) to accurately compare the magnitude of thickness change and fiber rotation across contraction of varying forces. Data used in regressions were pooled from all four individuals (Fig. 4). Regressions were performed in JMP (version 5.0; SAS Institute).

**ACKNOWLEDGMENTS.** We thank Drs. S. Gatesy and D. Baier for guidance on the development of muscle simulations and the Brown University Functional Anatomy and Biomechanics group for helpful comments on the manuscript. F. Nelson and T. Hsieh provided assistance during experiments. This work was supported in part by National Science Foundation Grants 0642428 (to T.J.R.) and 0629372 (to E.L.B.) and by a Bushnell Faculty Research Grant (to T.J.R.).

1. Biewener AA, Farley CT, Roberts TJ, Temaner M (2004) *J Appl Physiology* 97:2266–2274.
2. Carrier DR, Heglund NC, Earls KD (1994) *Science* 265:651–653.
3. Brainerd EL, Azizi E (2005) *J Exp Biol* 208:3249–3261.
4. Gans C, Bock W (1965) *Ergeb Anat Entw Gesch* 38:115.
5. Steno N (1667) *Elementorum Myologiae Specimen, seu Musculi Descripto Geometrica* (Florence, Italy).
6. Alexander RM (1968) *Animal Mechanics* (Sidgwick and Jackson, London).
7. Lieber RL, Friden J (2000) *Muscle Nerve* 23:1647–1666.
8. Muhl ZF (1982) *J Morphol* 173:285–292.
9. Maganaris CN, Baltzopoulos V, Sargeant AJ (1998) *J Physiol* 512:603–614.
10. Zuurbier CJ, Huijing PA (1992) *J Biomech* 25:1017–1026.
11. Baskin RJ, Paolini PJ (1967) *Am J Physiol* 213:1025.
12. Alexander RM (1998) *J Physiol* 512:315.
13. Otten E (1988) in *Exercise and Sports Sciences Reviews*, ed Pandolf KB (Macmillan, New York), Vol 16, pp 89–137.
14. Herbert RD, Gandevia SC (1995) *J Physiol* 484:523–532.
15. Hodges PW, Pengel LHM, Herbert RD, Gandevia SC (2003) *Muscle Nerve* 27:682–692.

16. Kubo K, Kawata T, Ogawa T, Watanabe M, Sasaki K (2006) *Arch Oral Biol* 51:146–153.
17. Hodgson JA, Finni T, Lai AM, Edgerton VR, Sinha S (2006) *J Morphol* 267:584–601.
18. Rome LC, Funke RP, Alexander RM, Lutz G, Aldridge H, Scott F, Freadman M (1988) *Nature* 335:824–827.
19. Rome LC, Lindstedt SL (1997) in *Handbook of Physiology, Section 13, Comparative Physiology*, ed Dantzler WH (Am Physiol Soc, Washington, DC), pp 1587–1651.
20. Huxley AF (1957) *Prog Biophys Chem* 7:255–318.
21. Scott SH, Brown IE, Loeb GE (1996) *J Muscle Res Cell Motil* 17:207–219.
22. Azizi E, Gillis GB, Brainerd EL (2002) *Comp Biochem Physiol A* 133:967–978.
23. Scott SH, Loeb GE (1995) *J Morphol* 224:73–86.
24. Donkelaar CCV, Willems PJB, Muijtjens AMM, Drost MR (1999) *J Biomech* 32:755–762.
25. Maganaris CN, Kawakami Y, Fukunaga T (2001) *J Anat* 199:449–456.
26. Van Leeuwen JL, Spoor CW (1992) *Phil Trans R Soc London Ser B* 336:275–292.
27. Van Leeuwen JL, Spoor CW (1993) *Phil Trans R Soc London Ser B* 342:321–333.
28. Purcell TJ, Morris C, Spudich JA, Sweeney HL (2002) *Proc Natl Acad Sci USA* 99:14159.
29. Nelson FE, Gabaldon AM, Roberts TJ (2004) *Comp Biochem and Physiol A* 37:711–721.